Animal Nutrition 14 (2023) 56–66

Contents lists available at ScienceDirect

Animal Nutrition

journal homepage: http://www.keaipublishing.com/en/journals/aninu/

Original Research Article

Uridine alleviates high-carbohydrate diet-induced metabolic syndromes by activating sirt1/AMPK signaling pathway and promoting glycogen synthesis in Nile tilapia (*Oreochromis niloticus*)

Nan-Nan Zhou, Tong Wang, Yu-Xin Lin, Rong Xu, Hong-Xia Wu, Fei-Fei Ding, Fang Qiao, Zhen-Yu Du, Mei-Ling Zhang*

Laboratory of Aquaculture Nutrition and Environmental Health (LANEH), School of Life Sciences, East China Normal University, Shanghai 200241, China

ARTICLE INFO

Article history:
Received 28 October 2022
Received in revised form
6 January 2023
Accepted 21 March 2023
Available online 3 May 2023

Keywords:
Uridine
High-carbohydrate diet
Metabolism
AMPK
Nile tilapia

ABSTRACT

Carbohydrates have a protein sparing effect, but long-term feeding of a high-carbohydrate diet (HCD) leads to metabolic disorders due to the limited utilization efficiency of carbohydrates in fish. How to mitigate the negative effects induced by HCD is crucial for the rapid development of aquaculture. Uridine is a pyrimidine nucleoside that plays a vital role in regulating lipid and glucose metabolism, but whether uridine can alleviate metabolic syndromes induced by HCD remains unknown. In this study, a total of 480 Nile tilapia (*Oreochromis niloticus*) (average initial weight 5.02 ± 0.03 g) were fed with 4 diets, including a control diet (CON), HCD, HCD + 500 mg/kg uridine (HCUL) and HCD + 5,000 mg/kg uridine (HCUH), for 8 weeks. The results showed that addition of uridine decreased hepatic lipid, serum glucose, triglyceride and cholesterol ($P < 0.05$). Further analysis indicated that higher concentration of uridine activated the sirtuin1 (sirt1)/adenosine 5-monophosphate-activated protein kinase (AMPK) signaling pathway to increase lipid catabolism and glycolysis while decreasing lipogenesis ($P < 0.05$). Besides, uridine increased the activity of glycogen synthesis-related enzymes ($P < 0.05$). This study suggested that uridine could alleviate HCD-induced metabolic syndrome by activating the sirt1/AMPK signaling pathway and promoting glycogen synthesis. This finding reveals the function of uridine in fish metabolism and facilitates the development of new additives in aquatic feeds.

1. Introduction

Carbohydrate is the main energy source for animals to sustain their life activities (Jéquier, 1994). An optimal level of carbohydrate in the diet can improve growth performance of fish and has a protein sparing effect (Zhao et al., 2020). However, the utilization efficiency of carbohydrate in fish is limited, and long-term intake of a high-carbohydrate diet (HCD) can be detrimental to fish health (Panserat and Kaushik, 2002). For example, it has been found that blunt snout bream (*Megalobrama amblycephala*) fed with HCD showed higher hepatosomatic index (HSI), intraperitoneal fat ratio and whole-body lipid content (Shi et al., 2018). Similarly, the study on Nile tilapia (*Oreochromis niloticus*) has shown that long-term feeding of HCD led to excessive hepatic lipid deposition and higher serum glucose content (Xu et al., 2022b). HCD could also cause oxidative stress in Nile tilapia (Xu et al., 2022a) and suppress innate immunity of juvenile largemouth bass (*Micropterus salmoides*) (Lin et al., 2018). In recent years, how to mitigate the metabolic disorders caused by HCD has received more and more attention. The research in blunt snout bream reported that the supplementation of metformin in HCD could activate adenosine 5-monophosphate-activated protein kinase (AMPK) to enhance insulin sensitivity and reduce plasma level of glucose (Xu et al., 2018). Besides, the research in *Lateolabrax japonicus* demonstrated that the supplementation of condensed tannins in HCD could increase weight gain ratio (WGR) and up-regulate the expression level of

* Corresponding author.
E-mail address: mlzhang@bio.ecnu.edu.cn (M.-L. Zhang).
Peer review under responsibility of Chinese Association of Animal Science and Veterinary Medicine.

Production and Hosting by Elsevier on behalf of KeAi

https://doi.org/10.1016/j.aninu.2023.03.010

hepatic glycolysis to decrease the serum glucose concentration (Peng et al., 2020). Moreover, probiotics or prebiotics were also used to regulate the metabolic syndrome induced by HCD. For example, supplementation of inulin could alleviate the metabolic syndrome by changing the intestinal bacterial composition in Nile tilapia fed with HCD (Wang et al., 2021). *Bacillus amyloliquefaciens* ameliorated HCD-induced lipid deposition and improved the glucose tolerance by increasing insulin sensitivity (Xu et al., 2022b).

Nucleosides are a class of low molecular compounds. They play essential roles in several biological processes, including transmitting genetic information, improving growth performance, boosting immunity and regulating metabolism in animals (Daneshmand et al., 2017; Liu et al., 2021). Uridine is the dominant nucleoside in plasma compared with other purine and pyrimidine nucleosides (Michailidou et al., 2020; Yamamoto et al., 2011). Uridine belongs to pyrimidine nucleosides and is an important building block of RNA. A study in mice has demonstrated that uridine was synthesized in liver and adipose tissues and then transferred to other tissues through vascular circulation (Deng et al., 2017). Uridine plays a crucial role in maintaining lipid and glucose homeostasis. Other studies in mice have demonstrated that uridine could prevent drug-induced hepatic lipid accumulation (Le et al., 2014a, 2014b). It has been found that activation of endogenous production of uridine in adipocytes promoted lipolysis to protect mice from obesity (Deng et al., 2018). Depletion of uridine in serum and liver led to the accumulation of hepatic lipid, which could be alleviated by supplementing uridine in the diet (Le et al., 2013). Furthermore, uridine metabolites can combine with glucose to form pyrimidine–sugar conjugates to participate in glycogen synthesis (Yamamoto et al., 2011). A previous study also reported that oral uridine administration could improve glucose tolerance in mice fed with a high-fat diet (Deng et al., 2017). However, long-term feeding of uridine could induce hepatic lipid accumulation and systemic glucose intolerance in mice (Urasaki et al., 2016), suggesting the function of uridine still needs further investigation. Moreover, whether uridine can regulate glucose and lipid metabolism remains unknown in fish.

As an economic fish of great importance, Nile tilapia ranks among the top 3 in global finfish aquaculture production, which makes it indispensable for the world's protein supply (FAO, 2022). Previous study reported that the optimal carbohydrate level in tilapia fingerlings diet is 30% to 40% (Ali and Al-Asgah, 2001). In this study, the accumulation of lipid in the liver and an elevated glucose, triglyceride and total cholesterol content in serum were observed in fish fed with HCD, and the effects of uridine on lipid and glucose metabolism and the possible mechanisms were further investigated.

2. Materials and methods

2.1. Ethics statement

This experiment was performed according to the guidelines for the care and use of laboratory experimental animals in China. This research was approved by the Committee on the Ethics of Animal Experiments of East China of Normal University (F20201002).

2.2. Experimental diets

Four purified isolipidic and isonitrogenous feeds were formulated, including a control diet (CON), high-carbohydrate diet (HCD), HCD supplemented with 500 mg/kg uridine (Macklin, Shanghai, China) (HCUL), and HCD supplemented with 5,000 mg/kg uridine (HCUH). In all diets, gelatin and casein were used as protein sources. Soybean oil served as the lipid source and corn starch was the main carbohydrate source. The ingredients and proximal composition of the experimental diets are shown in Table 1. All ingredients were ground into powder and mixed thoroughly by a feed mixer. Soybean oil and water were incorporated with the mixture to form a dough, and then pelleted by using a screw-press pelletizer (F-26, South China University of Technology, Guangzhou, China). The feeds were dried at room temperature for approximately 3 days. After drying, all diets were stored at −20 °C until use.

2.3. Experiment design and feeding management

Juvenile Nile tilapias were purchased from Guangzhou Tianfa Fishery Development Co. Ltd. (Guangzhou, China). Before the experiment, all fish were raised in the circulating culture system to acclimate to the experimental conditions for 2 weeks. After acclimation, a total of 480 visually healthy juvenile Nile tilapias (average initial weight, 5.02 ± 0.03 g) were selected and randomly distributed to 12 tanks (200 L, 60 cm × 60 cm × 65 cm) in triplicate (40 fish per tank). The water flow rate in the recirculating culture system was 0.6 L/min. During the feeding trial, all fish were fed twice daily (08:30 and 17:30) for 8 weeks at a feeding rate of 4% body weight. Each morning, the oxygen supply was temporarily stopped before feeding and the feces were pumped out with a pumping tube. The total weight of fish in each tank was measured

Table 1
Ingredients and proximate chemical composition of the experimental diets.

Item	CON	HCD	HCUL	HCUH
Ingredients, g/kg				
Casein[1]	320	320	320	320
Gelatin[2]	80	80	80	80
Soybean oil[3]	70	70	70	70
Corn starch[4]	300	450	450	450
Mineral premix[5]	10	10	10	10
Vitamin premix[6]	10	10	10	10
$Ca(H_2PO_4)_2$[7]	10	10	10	10
Carboxymethyl cellulose[8]	25	25	25	25
Uridine[9]	0	0	0.5	5
Cellulose[10]	167.75	17.75	17.25	12.75
Choline chloride[11]	5	5	5	5
Dimethyl-beta-propiothetin[12]	2	2	2	2
Butylated hydroxytoluene[13]	0.25	0.25	0.25	0.25
Total	1,000	1,000	1,000	1,000
Proximate composition, g/kg dry matter				
Crude lipid	64	62	67	68
Crude protein	356	354	355	349
Moisture	111	122	120	126
Ash	31.3	33.6	33.8	32.6

CON = control diet; HCD = high-carbohydrate diet; HCUL = high-carbohydrate diet + 500 mg/kg uridine; HCUH = high-carbohydrate diet + 5,000 mg/kg uridine.
[1] Casein: Gansu Hualing Dairy Co., Ltd., China.
[2] Gelatin: Sangon Biotech (Shanghai) Co., Ltd., China.
[3] Soyben oil: Yihai Kerry Arawana Holdings Co., Ltd., China.
[4] Corn starch: Shandong Hengren Industry and Trade Co., Ltd., China.
[5] Mineral premix (Hangzhou Minsheng Bio-Tech Co., Ltd., China) (g/kg mineral premix): 314.0 $CaCO_3$; 469.3 KH_2PO_4; 147.4 $MgSO_4 \cdot 7H_2O$; 49.8 NaCl; 10.9 Fe (II) gluconate; 3.12 $MnSO_4 \cdot H_2O$; 4.67 $ZnSO_4 \cdot 7H_2O$; 0.62 $CuSO_4 \cdot 5H_2O$; 0.16 KI; 0.08 $CoCl_2 \cdot 6H_2O$; 0.06 $(NH_4)_2MoO_4$; 0.02 $NaSeO_3$.
[6] Vitamin premix (Hangzhou Minsheng Bio-Tech Co., Ltd., China) (mg or IU/kg vitamin premix): 500,000 I.U. (international units) vitamin A; 50,000 I.U. vitamin D_3; 2,500 mg vitamin E; 1,000 mg vitamin K_3; 5,000 mg vitamin B_1; 5,000 mg vitamin B_2; 5,000 mg vitamin B_6; 5,000 μg vitamin B_{12}; 25,000 mg inositol; 10,000 mg pantothenic acid; 100,000 mg choline; 25,000 mg niacin; 1,000 mg folic acid; 250 mg biotin; 10,000 mg vitamin C.
[7] $Ca(H_2PO_4)_2$: Sangon Biotech (Shanghai) Co., Ltd., China.
[8] Carboxymethyl cellulose: Shandong Dongda Commerce Co., Ltd., China.
[9] Uridine: Macklin Biochemical Technology Co., Ltd., China.
[10] Cellulose: Shandong Dongda Commerce Co., Ltd., China.
[11] Choline chloride: Sangon Biotech (Shanghai) Co., Ltd., China.
[12] Dimethyl-beta-propiothetin: Beijing Greenfocus Technology Co., Ltd., China.
[13] Butylated hydroxytoluene: Sangon Biotech (Shanghai) Co., Ltd., China.

every 2 weeks and the feeding consumption was adjusted according to the weight. During the 8-week trial, fish were reared on a 12 h:12 h light:dark photoperiod. The water temperature was maintained at 28 ± 1.0 °C while the dissolved oxygen and pH varied from 7.0 to 7.9 mg/L and 7.2 to 7.8, respectively.

2.4. Sample collection

At the end of the 8-week trial, all fish were fasted for 24 h before sampling. Fish from each tank were counted and group-weighed to determine the final weight and calculate the WGR. The feed conversion ratio (FCR) was calculated based on the amount of feed fed in each tank and the weight gain of fish in each tank. Twelve fish from each treatment (4 fish per tank) were randomly selected and euthanized with MS-222 (20 mg/L, tricaine methane sulfonate, Western Chemicals Inc., USA). The body length and weight of 12 fish were measured individually to calculate the condition factor (CF). Blood was sampled from the caudal vertebral vein by using a 1-mL sterile syringe (Klmedical, China) and then centrifuged for serum preparation (1,200 × *g* at 4 °C for 10 min). Serum was immediately stored at −80 °C until use. Viscera and liver tissues were dissected and weighted for the calculation of viscerosomatic index (VSI) and HSI. Additionally, the dissected muscle and liver tissues were immediately frozen in liquid nitrogen and kept at −80 °C for future analysis. The WGR, FCR, CF, VSI and HSI were calculated using the following formulae:

Weight gain ratio (%) = 100 × (final fish weight − initial fish weight)/initial fish weight,

Feed conversion ratio = total feed fed in each tank/(total final fish weight in each tank − total initial fish weight in each tank),

Condition factor (g/cm^3) = 100 × (final fish weight/final fish $length^3$),

Viscerosomatic index (%) = 100 × (viscera weight/body weight),

Hepatosomatic index (%) = 100 × (liver weight/body weight).

2.5. Proximate composition analysis of diets and whole fish

Proximate composition of the experimental diets and whole fish body were analyzed according to Association of Official Analytical Chemists (AOAC, 2005). Six fish per treatment (2 fish per tank) were randomly selected for body composition analysis. In brief, moisture content was detected by drying the samples to a constant weight at 105 °C. The total protein of whole fish was determined by a semi-automatic Kjedahl System (FOSS, Sweden) after acid digestion. The total lipid of whole fish and liver were determined following homogenization with chloroform-methanol solution (2:1, vol:vol) as previously described (Folch et al., 1957). The ash content was measured using a muffle furnace at 550 °C for 6 h.

2.6. Biochemical analysis

The triglyceride (TG), total cholesterol (TC) contents in serum and liver were determined by using biochemical assay kits (Cat No. A110-1-1 and A111-1-1) (Jiancheng Biotech Co., Ltd., China) based on relevant kit protocols. Glucose content and the activity of aspartate aminotransferase (AST), alanine aminotransferase (ALT) in serum were measured using biochemical assay kits (Cat No. F006-1-1, C010-2-1 and C009-2-1) (Jiancheng Biotech Co., Ltd., China) according to the manufacturer's instructions. The content of glycogen in liver and muscle was determined using biochemical assay kits (Beijing Solarbio Science & Technology Co., Ltd., China) (Cat No. BC0340) following the manufacture's protocols. The activities of glycogen synthase, glycogen phosphorylase, uridine−cytidine kinase 1 (Uck1) and cytidine/uridine monophosphate kinase 1 (Cmpk1) were measured by enzyme linked immunosorbent assay (ELISA) kit (Shanghai Hengyuan Biological Technology Co., Ltd., China).

2.7. Histochemical staining

The liver and muscle tissues were fixed in 4% paraformaldehyde (Servicebio, China) and then embedded in paraffin. Oil red O staining and PAS staining were performed using the standard protocols on 5-μm thickness tissue sections. Histology images were observed and captured under a light microscope (Nikon Corporation, Japan).

2.8. Nile tilapia primary hepatocytes culture and pharmacological inhibition

Nile tilapia primary hepatocytes were isolated and cultured according to Jiao et al. (2020). Briefly, liver tissue was washed three times with 1× PBS, cut up with scissors and digested with L-15 Leibovitz medium (Cytiva, USA) containing 0.1% collagenase IV (Gibco, USA). The mixture was filtered through a 70-μm nylon mesh and the cells were collected by centrifugation at 800 × *g* for 10 min. Red cells were removed using red cell lysis buffer (Tiangen, China), and the remaining hepatocytes were cultured in L-15 Leibovitz medium with 1% penicillin−streptomycin and 10% fetal bovine serum (FBS, Gibco, USA) at 28 °C. Cells were treated with uridine (500 μM uridine) and nicotinamide with the final concentration at 0.5, 1 and 2 μM, referred to as UNL, UNM and UNH groups, respectively. After 24 h of incubation, cells were collected to detect the expression of sirtuin1 (*sirt1*), AMP-activated protein kinase alpha 1 (*ampkα1*) and AMP-activated protein kinase alpha 2 (*ampkα2*).

2.9. RNA isolation and quantitative real-time PCR

Total RNA was isolated using Trizol reagent from 50 to 100 mg tissues following the manufacturer's instructions (Aidlab, China). The quality and concentration of the extracted RNA were assessed by 1% agarose gel electrophoresis and a Nanodrop 2000C spectrophotometer (Thermo Fisher Scientific, USA). The isolated RNA (1 μg) was used for reverse transcription with an RT reagent Kit (Vazyme Biotech Co., Ltd, China) by Thermal Cycler (Bio-Rad, USA). The primers used for quantitative real-time PCR (qPCR) in this study were designed in the National Center for Biotechnology Information (NCBI), the amplification efficiency of each gene ranged from 90% to 105%, and the correlation coefficient of each gene was greater than 0.98 (Table 2). The amplicon size ranged from 90 to 180 bp. The qPCR was performed in a CFX96 real-time PCR detection system. The qPCR reaction solution contained 5 μL of ChamQ Universal SYBR qPCR Master Mix (Vazyme Biotech Co., Ltd., China), 0.5 μL of 2.5 μM forward and reverse primers, 1 μL of cDNA template and 3 μL of nuclease-free water. The qPCR conditions consisted of 1 cycle at 95 °C for 30 s followed by 40 cycles at 95 °C for 5 s and an annealing step at 60 °C for 15 s. The melting curves of the amplified products were performed (95 °C for 15 s, 60 °C for 1 min and 95 °C for 15 s) to ensure the specificity of the primers. β-Actin and elongation factor 1 alpha (*ef1α*) genes were used for normalization. The relative expression level was determined using the $2^{-\Delta\Delta CT}$ method.

Table 2
The primer sequences used in the experiment.

Gene	Forward primer (5′ to 3′)	Reverse primer (5′ to 3′)	GenBank no.
β-Actin	AGCCTTCCTTCCTTGGTATGGAAT	TGTTGGCGTACAGGTCCTTACG	XM_003443127.5
ef1α	ATCAAGAAGATCGGCTACAACCCT	ATCCCTTGAACCAGCTCATCTTGT	NM_001279647.1
accα	TAGCTGAAGAGGAGGGTGCAAGA	AACCTCTGGATTGGCTTGAACA	XM_005471970
Fas	TCATCCAGCAGTTCACTGGCATT	TGATTAGGTCCACGGCCACA	XM_003454056.5
dgat2	GCTTGAATTCTGTCACCCTGAAGA	ACCTGCTTGTAGGCGTCGTTCT	XM_003458972
atgl	GACACATGCTGCAAAGCACT	ACCAGGACGTTTTCTCCGTC	XM_003440346.5
hsl	AGTTCACTCCAGCCATTCGG	TGGCTGCTACCCCTATTCCT	XM_005463937.4
cpt1a	TTTCCAGGCCTCCTTACCCA	TTGTACTGCTCATTGTCCAGCAGA	XM_003440552
aco	AGTCCCACTGTGAGCTCCATCAA	CAGACCATGGCAGTTTCCAAGA	XM_003447910.5
pparα	GTTCCTCAAGAGTCTCCGCC	AAAGAGCTAGGTCGCTGTCG	XM_005455554.4
gck	GACATGAGGACATTGACAAGGGAA	CTTGATGGCGTCTCTGAGTAAACC	XM_003451020.2
pfk	AACCTGTGTGTGATTGGAGGTGAT	CGTGATCTTACCGGCTTTAACAAG	XM_003441476.2
pk	CAGCATAATCTGCACCATCGGT	ATGAGAGAAGTTAAGACGGGCGA	XM_005472621.3
pc	ATGTCACACCCGATGCTTCC	ATATCGTCTGAACGCCTGCC	XM_003452415.5
pepck	TGGAAGAACAAACCTTGGCG	TGGGTCAATAATGGGACACTGTCT	XM_003448375
fbpase	ACCGGACAATAGCGGAAAATACA	TGGCGAATATTGTTCCTATGGAGA	XM_003449650.4
ugp2	ATCGACAATCTGGGAGCCAC	GCGCAGCTTCCCTTCATACT	XM_003451454.5
sirt1	AGACGTTGCTGGATGAGTCG	AACAGGTATTGGCCTGCCTC	XM_003437795.3
ampkα1	GCATCATGAGCGAAGCCAAG	AGTCTCCGCCACGAGAAAAG	NM_001319868.1
ampkα2	TGACAGGCCATAAAGTGGCT	CGGTGTGCTTATGACCTGGTA	NM_001319869.1

ef1α = ongationfactor1-alpha; *accα* = acetyl-CoA carboxylase alpha; *fas* = fatty acid synthase; *dgat2* = diacylglycerol O-acyl-transferase 2; *atgl* = adipose triglyceride lipase; *hsl* = hormone-sensitive lipase; *cpt1a* = carnitine palmitoyltransferase 1a; *aco* = acyl-coenzyme A oxidase; *pparα* = peroxisome proliferator activated receptor-alpha; *gck* = glucokinase; *pfk* = phosphofructokinase; *pk* = pyruvate kinase; *pc* = pyruvate carboxylase; *pepck* = phosphoenolpyruvate carboxykinase; *fbpase* = fructose-1,6-bisphosphate phosphatase; *ugp2* = uridyl diphosphate glucose pyrophosphorylase 2; *sirt1* = sirtuin 1; *ampkα1* = AMP-activated protein kinase alpha 1; *ampkα2* = AMP-activated protein kinase alpha 2.

2.10. Western blotting

RIPA (Beyotime Biotechnology, China) containing 1 mM PMSF (Beyotime Biotechnology, China) was used to homogenize liver tissue and then the mixture was incubated on ice for 30 min. Lysates were then centrifuged for 10 min at 14,000 × *g* at 4 °C. The concentration of protein in the supernatant was measured by bicinchoninic acid assay (BCA) (Beyotime Biotechnology, China). Equal amounts of protein were subjected to 10% ExpressCast PAGE Gels (Cat No. P2012) (New Cell & Molecular Biotech Co., Ltd, China) and then transferred onto a nitrocellulose membrane. The membrane was blocked with 5% BSA at 25 °C for 30 min and incubated with the appropriate primary antibody at 4 °C for 12 h. After washing with TBST, the membrane was incubated with the anti-Rabbit IgG. The anti-p-AMPK (Thr172, 1:800, Cat#2535, Cell Signaling Technology), anti-GAPDH (1:1,000, AB0036, Abways) were used to determine the expression of the corresponding proteins. GAPDH was used as an internal control to ensure equal protein loading. The protein bands were monitored using the Odyssey CLx Imager (Licor, USA). The target proteins were quantified using ImageJ software.

2.11. Statistical analysis

All data are represented as mean ± SEM. Normal distribution was tested using the Shapiro–Wilk test in GraphPad Prism 7.0 (GraphPad, USA). Statistical analysis was performed using GraphPad Prism 7.0, an independent-sample *t*-test was used to determine the differences between the 2 groups. The results with $P < 0.05$ values were considered statistically significant.

3. Results

3.1. Effects of uridine on the growth performance and body composition in Nile tilapia

After the 8 week feeding trial, the growth condition and body composition of fish were measured. As shown in Table 3, there was no significant difference in WGR, FCR, VSI, whole body composition

Table 3
Growth performance, biological indices and body composition of Nile tilapia fed different experiment diets.

Index	CON	HCD	HCUL	HCUH
Initial weight, g	5.02 ± 0.02	5.01 ± 0.01	5.03 ± 0.01	5.02 ± 0.01
Final weight, g	35.77 ± 0.76	36.53 ± 0.19	36 ± 0.43	36.52 ± 0.51
WGR, %	612.3 ± 14.75	632.7 ± 3.68	615.9 ± 8.75	627.7 ± 9.16
FCR	1.11 ± 0.01	1.08 ± 0.03	1.08 ± 0.02	1.10 ± 0.04
CF, g/cm^3	3.30 ± 0.08	3.65 ± 0.09$^{\#\#}$	3.40 ± 0.06*	3.44 ± 0.05*
VSI, %	10.53 ± 0.33	10.33 ± 0.43	10.73 ± 0.38	11.02 ± 0.34
HSI, %	2.16 ± 0.10	2.39 ± 0.05$^{\#}$	2.06 ± 0.10**	1.95 ± 0.07***
Whole body composition, % of wet weight				
Moisture	73.50 ± 0.24	73.35 ± 0.20	73.13 ± 0.21	73.14 ± 0.35
Total lipid	5.50 ± 0.29	5.55 ± 0.19	5.85 ± 0.18	5.97 ± 0.19
Total protein	13.96 ± 0.22	14.34 ± 0.12	13.91 ± 0.18	13.92 ± 0.20
Ash	2.62 ± 0.06	2.58 ± 0.04	2.53 ± 0.05	2.68 ± 0.13

CON = control diet; HCD = high-carbohydrate diet; HCUL = high-carbohydrate diet + 500 mg/kg uridine; HCUH = high-carbohydrate diet + 5,000 mg/kg uridine; WGR = weight gain ratio; FCR = feed conversion ratio; CF = condition factor; VSI = viscerosomatic index; HSI = hepatosomatic index. $n = 3$ for initial weight, final weight, WGR and FCR; $n = 12$ for CF, VSI, HSI; $n = 6$ for moisture, total lipid, total protein and ash. Data are represented as mean ± SEM. Significant difference between CON and HCD ($\#P < 0.05$, $\#\#P < 0.01$). Significant difference compared with HCD ($*P < 0.05$, $**P < 0.01$, $***P < 0.001$).

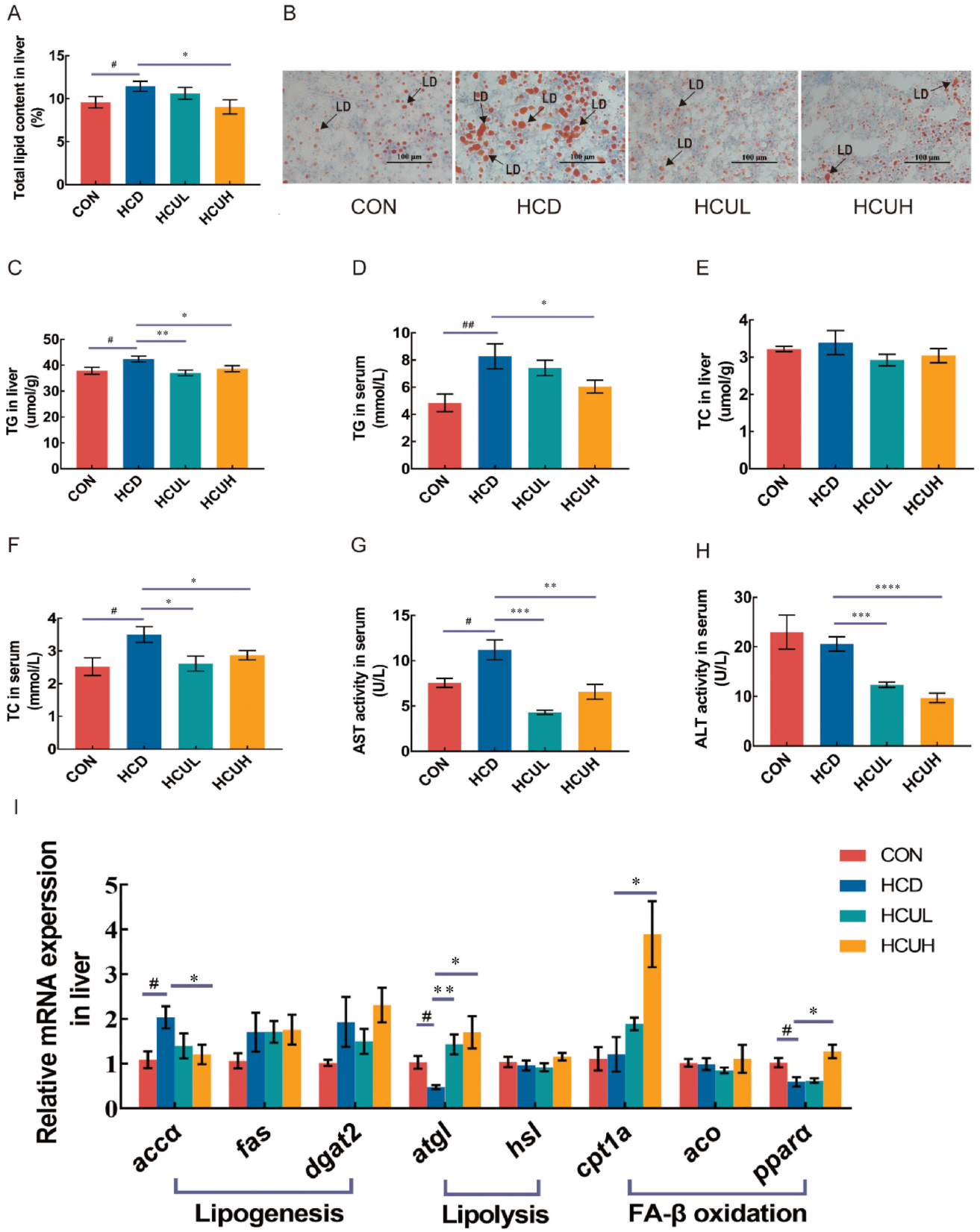

Fig. 1. The effect of uridine on the liver lipid metabolism of Nile tilapia. (A) Total lipid content in liver ($n = 12$). (B) Oil-red staining of liver. Scale bars = 100 μm. Arrow shows the stained red lipid drops in liver cells. (C) TG in liver ($n = 12$). (D) TG in serum ($n = 12$). (E) TC in liver ($n = 12$). (F) TC in serum ($n = 12$). (G) AST activity in serum ($n = 12$). (H) ALT activity in serum ($n = 12$). (I) mRNA expression of genes related to lipid metabolism ($n = 6$). Data are represented as mean ± SEM. Significant difference between CON and HCD (#$P < 0.05$, ##$P < 0.01$). Significant difference compared with HCD (*$P < 0.05$, **$P < 0.01$, ***$P < 0.001$, ****$P < 0.0001$). CON = control diet; HCD = high-carbohydrate diet; HCUL = high-carbohydrate diet + 500 mg/kg uridine; HCUH = high-carbohydrate diet + 5,000 mg/kg uridine; LD = lipid drop; TG = triglyceride; TC = total cholesterol; AST = aspartate aminotransferase; ALT = alanine aminotransferase; *accα* = acetyl-CoA carboxylase alpha; *fas* = fatty acid synthase; *dgat2* = diacylglycerol O-acyl-transferase 2; *atgl* = adipose triglyceride lipase; *hsl* = hormone-sensitive lipase; *cpt1a* = carnitine palmitoyltransferase 1a; *aco* = acyl-coenzyme A oxidase; *pparα* = peroxisome proliferator activated receptor-alpha.

between the CON and HCD groups, or between the HCD and uridine supplementation groups. The HCD group showed significant higher CF and HSI than CON, but addition of uridine significantly decreased these 2 parameters ($P < 0.05$). These results suggested that the addition of uridine to HCD had no effect on the growth performance or body composition, but decreased CF and HSI.

3.2. Uridine attenuated hepatic lipid accumulation in the HCD diet

Considering that the addition of uridine to HCD reduced HSI and CF, the total lipid content of the liver was measured. The result showed that the content of hepatic lipid in the HCD group was significantly higher than that in the CON group, but it was decreased significantly in the HCUH group ($P < 0.05$; Fig. 1A). The results of oil red O staining of liver showed an increased lipid droplet content in the HCD group compared with that in the CON group, and the lipid droplet content was significantly decreased in the HCUL and HCUH groups (Fig. 1B). The contents of TG and TC in liver and serum were quantified in the 4 groups. As shown in Fig. 1C, the liver TG in the HCD group was significantly higher than that in the CON group, but it was significantly decreased by the addition of uridine ($P < 0.05$). The serum TG was higher in the HCD group compared with the CON group, and it was decreased significantly in the HCUH group ($P < 0.05$; Fig. 1D). Liver TC did not change among treatments (Fig. 1E). However, compared with the CON group, the serum TC was significantly increased in the HCD group, and the addition of uridine significantly inhibited the increase of serum TC caused by HCD ($P < 0.05$; Fig. 1F). Considering that hepatic lipid accumulation can trigger hepatic injury (Musso et al., 2009), the activities of AST and ALT in serum, biomarkers of hepatic injury, were detected. The results showed that the serum AST activity increased significantly in the HCD group compared with the CON group, while uridine supplementation significantly decreased the serum AST activity ($P < 0.05$; Fig. 1G). Likewise, the serum ALT activity decreased significantly by the addition of uridine ($P < 0.05$; Fig. 1H).

The effect of uridine on the expression level of key genes related to lipid metabolism in liver was further detected (Fig. 1I). The expression level of genes, including fatty acid synthase (*fas*), diacylglycerol O-acyl-transferase 2 (*dgat2*), hormone-sensitive lipase (*hsl*) and acyl-coenzyme A oxidase (*aco*), showed no significant difference between the CON and HCD groups, or between the HCD and uridine supplemented groups. However, the expression level of acetyl-CoA carboxylase alpha (*acc*α), which is a rate-limiting enzyme for lipogenesis, was significantly increased in the HCD group compared with the CON group ($P < 0.05$; Fig. 1I). In addition, the expression levels of adipose triglyceride lipase (*atgl*) and peroxisome proliferator activated receptor-alpha (*ppar*α), which are involved in lipolysis and fatty acid β oxidation respectively, were significantly inhibited by HCD diet ($P < 0.05$; Fig. 1I). Interestingly, HCUH group reduced the expression level of *acc*α and increased the expression level of *atgl*, carnitine palmitoyltransferase 1a (*cpt1a*) and *ppar*α significantly compared with the HCD group ($P < 0.05$; Fig. 1I). Collectively, these data further demonstrated that uridine could alleviate liver lipid accumulation caused by HCD diet by inhibiting lipogenesis and promoting lipolysis and fatty acid β oxidation.

3.3. Uridine improved glucose metabolism and promoted glycogen accumulation

A high-carbohydrate diet tends to cause glucose metabolism disorder in fish (Xu et al., 2022b). In order to investigate the effect of uridine on glucose metabolism, the serum glucose in the 4 groups were measured. The serum glucose in the HCD group was significantly higher than the CON group, while uridine supplementation remarkably reduced the serum glucose ($P < 0.05$; Fig. 2A). The glycogen content in muscle and liver were also detected. The HCUH group exhibited higher liver glycogen content than the HCD group ($P < 0.05$; Fig. 2B). The glycogen content in muscle was significantly increased by the addition of uridine ($P < 0.05$; Fig. 2C). A significant increase in glycogen granules was found in the liver of the HUCH group and in the muscle of the HCUL and HCUH groups by PAS staining (Fig. 2D). The effect of uridine on the expression level of genes related to glycolysis and gluconeogenesis in liver was detected. The results showed the expression level of genes related to glycolysis (glucokinase [*gck*] and phosphofructokinase [*pfk*]) or gluconeogenesis (pyruvate carboxylase [*pc*] and fructose-1,6-bisphosphate phosphatase [*fbpase*]) was inhibited in the HCD group compared with the CON group ($P < 0.05$; Fig. 2E). However, the HCUH group increased the expression level of glycolysis related genes, including *gck*, *pfk* and pyruvate kinase (*pk*), significantly ($P < 0.05$; Fig. 2E). The influence of uridine on glycogen metabolism was further explored. The results showed that uridine supplementation significantly increased the glycogen synthetase activity in liver ($P < 0.05$; Fig. 2F). However, the glycogen phosphorylase activity in the liver was not affected by HCD or addition of uridine ($P < 0.05$; Fig. 2G). In addition, the expression level of uridyl diphosphate glucose pyrophosphorylase 2 (*ugp2*), which is the key gene related to glycogen synthesis, decreased significantly in liver in the HCD group compared with the CON group but increased in the HCUH group ($P < 0.05$; Fig. 2H). Compared with the HCD group, uridine supplementation significantly increased the activity of glycogen synthetase and glycogen phosphorylase in muscle ($P < 0.05$; Fig. 2I and J). In addition, the expression level of *ugp2* in muscle was also up-regulated in the HCUH group ($P < 0.05$; Fig. 2K). These results showed that the addition of uridine reduced the serum glucose, activated glycolysis in the liver and promoted glycogen synthesis in liver and muscle.

Considering that uridine triphosphate (UTP), the metabolite of uridine, is a substrate for glycogen synthesis, the activity of key enzymes for the metabolism of uridine to UTP (Uck1; Cmpk1) were also examined. The results showed that different dietary treatments had no significant effect on the activity of Uck1 in liver (Fig. 3A). However, the HCUH group significantly increased the activity of Cmpk1 in liver compared with the HCD diet ($P < 0.05$; Fig. 3B). In muscle, the activity of Uck1 was increased significantly in the HCUH group compared with the HCD group ($P > 0.05$; Fig. 3C), and Cmpk1 activity was significantly increased in the uridine addition groups compared with the HCD group ($P < 0.05$; Fig. 3D). These data demonstrated that the addition of higher concentration of uridine activated the transformation of uridine to UTP in liver and muscle.

3.4. Uridine activated AMPK phosphorylation by activating sirt1

A previous study reported that glucose and lipid metabolism were regulated by AMPK phosphorylation (Cool et al., 2006). In order to further investigate whether uridine could affect the phosphorylation of AMPK, we measured the p-AMPK protein expression level in the liver. HCUH increased the p-AMPK protein expression level significantly compared with the HCD diet ($P < 0.05$; Fig. 4A and B). Consistent with the activation of AMPK, the expression level of *sirt1* in the liver was up-regulated by the HCUH group ($P < 0.05$; Fig. 4C). To further confirm whether *sirt1* is required for AMPK activation, we treated tilapia primary hepatocytes with nicotinamide (an inhibitor of sirt1). The results showed that the addition of uridine could activate the expression level of *sirt1*, *ampk*α*1* and *ampk*α*2* significantly ($P < 0.05$; Fig. 4D–F). However, the activation effect of uridine was abolished in the presence of nicotinamide (Fig. 4D–F).

4. Discussion

Uridine is a pyrimidine nucleoside necessary for life activities and plays an important role in the metabolic processes of animals (Zhang et al., 2020). A large number of studies in mammals have shown that uridine could promote intestinal health (Wu et al., 2020), influence glucose and lipid metabolism and enhance growth performance (Deng et al., 2017; Gao et al., 2021; Peng et al., 2013), but whether uridine can influence the growth performance and metabolic characteristics in fish fed with a HCD has not been reported. In the present study, the WGR and body composition of Nile tilapia were not affected by uridine supplementation. Although

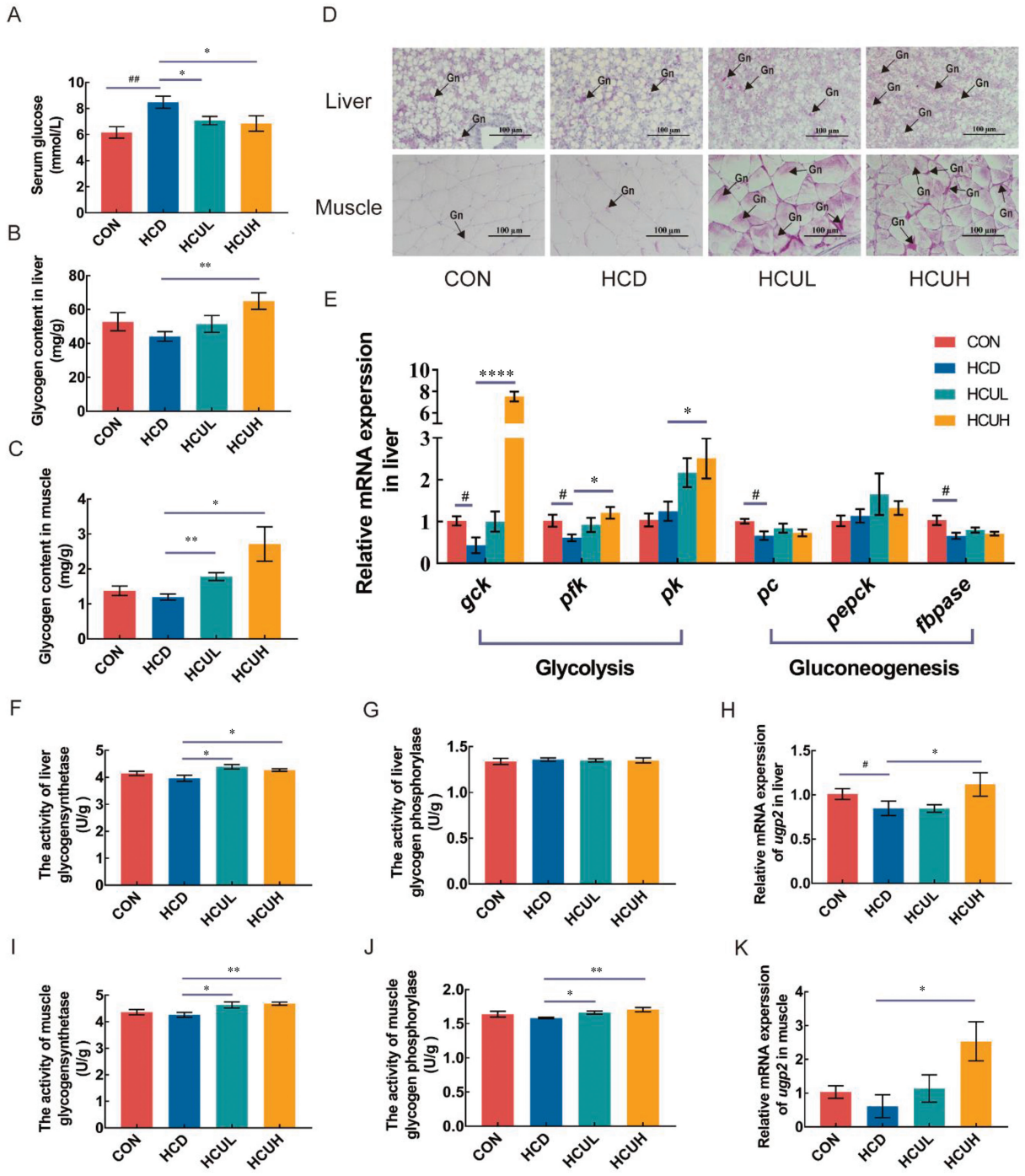

Fig. 2. The effect of uridine on liver and muscle glucose metabolism of Nile tilapia. (A) Serum glucose ($n = 12$). (B) Glycogen content in liver ($n = 6$). (C) Glycogen content in muscle ($n = 6$). (D) PAS staining of liver and muscle. Scale bars = 100 μm. Arrow shows the stained fuchsia glycogen granule in liver and muscle cells. (E) mRNA expression of genes related to glucose metabolism in liver ($n = 6$). (F) The activity of liver glycogen synthetase ($n = 6$). (G) The activity of liver glycogen phosphorylase ($n = 6$). (H) mRNA expression of *ugp2* in liver ($n = 6$). (I) The activity of muscle glycogen synthetase ($n = 6$). (J) The activity of muscle glycogen phosphorylase ($n = 6$). (K) mRNA expression of *ugp2* in muscle ($n = 6$). Data are represented as mean ± SEM. Significant difference between CON and HCD (#$P < 0.05$, ##$P < 0.01$). Significant difference compared with HCD (*$P < 0.05$, **$P < 0.01$, ****$P < 0.0001$). CON = control diet; HCD = high-carbohydrate diet; HCUL = high-carbohydrate diet + 500 mg/kg uridine; HCUH = high-carbohydrate diet + 5,000 mg/kg uridine; Gn = glycogen; *gck* = glucokinase; *pfk* = phosphofructokinase; *pk* = pyruvate kinase; *pc* = pyruvate carboxylase; *pepck* = phosphoenolpyruvate carboxykinase; *fbpase* = fructose-1,6-bisphosphate phosphatase; *ugp2* = uridyl diphosphate glucose pyrophosphorylase 2.

the effect of uridine on fish growth performance has not been reported, the influence of other nucleotides on the growth performance remains inconsistent. It has been shown that nucleotide supplementation had no effect on specific growth rate of juvenile turbot (Peng et al., 2013). Dietary nucleotide supplementation did not exert beneficial effects on the growth performance of channel catfish and red drum (Cheng et al., 2011; Welker et al., 2011). However, it has been found that dietary nucleotide supplementation could improve the growth performance in rainbow trout and grouper (Lin et al., 2009; Tahmasebi-Kohyani et al., 2011). Different dietary patterns, fish species, fish developmental stages and nucleotide concentrations may be possible reasons for the inconsistency. The growth promoting effect of uridine still needs further investigation in different fish species.

A previous study has shown that uridine could alleviate obesity induced by a high-fat diet in mice (Liu et al., 2021). Condition factor is an indicator of the fatness of fish, and our results showed that the supplementation of uridine significantly attenuated the increase of CF in Nile tilapia caused by a HCD, which was consistent with the effect of uridine reported in mice (Liu et al., 2021). HSI could provide a reliable assessment of the overall growth and health status of fish (Du and Turchini, 2021). Accumulation of hepatic lipid is usually accompanied by an increase in HSI (Liu et al., 2010; Xu et al., 2022b). In the present study, uridine significantly inhibited the increase of HSI caused by a HCD diet. In the HCUL and HCUH groups, less lipid accumulation was observed and lower lipid content was detected, indicating a reduction of lipid accumulation in the liver by dietary uridine supplementation. Further analysis showed that the addition of higher concentrations of uridine significantly inhibited the expression of lipogenesis genes (*accα*) and up-regulated the expression of genes related to lipolysis (*atgl*) and fatty acid-β oxidation (*cpt1a*, *pparα*). In agreement with our results, a study in pigs showed that uridine supplementation down-regulated the expression of *acc* and activated the expression of *hsl* and *pparα* (Gao et al., 2021). Taken together, these results indicated that the addition of uridine alleviated hepatic lipid accumulation caused by a HCD diet by suppressing the synthesis of liver lipid and promoting lipid catabolism in the liver.

AMPK is an energy sensor that maintains cell energy homeostasis (Kahn et al., 2005) and plays an important role in regulating the homeostasis of lipid metabolism (Li et al., 2011). Activation of AMPK has long been proposed as a valuable target for the treatment of metabolic diseases (Carling, 2017; Day et al., 2017). It has been found that the activation of AMPK in the liver inhibited *accα* gene expression and upregulated the gene expression level of *atgl*, *cpt1a* and *pparα*, resulting in a significant reduction in liver and serum lipid content in mice (Takikawa et al., 2010; Yao et al., 2018), which is consistent with our results. A previous study showed that supplementation with uridine could inhibit fatty liver development by increasing the NAD^+/NADH ratio and modulating the protein acetylation profile of metabolic in mice (Le et al., 2013). It is known that Sirt1 is an evolutionary conserved NAD^+-dependent deacetylase. Sirt1 senses the concentration of intracellular NAD^+ and is involved in the metabolic regulation of the cell (Cantó and Auwerx, 2012). A previous study showed that Sirt1 promoted the phosphorylation of AMPK by deacetylating the upstream kinase of AMPK (Liang et al., 2014). Other studies also showed Sirt1 could regulate hepatocyte lipid metabolism by activating AMPK phosphorylation (Yao et al., 2018). In agreement, our results showed that uridine supplementation activated the expression of *sirt1*. It has been demonstrated that *sirt1* overexpression could activate the phosphorylation of AMPK in 293T cells, in contrast, short hairpin RNA for *sirt1* had the opposite effect on the phosphorylation of AMPK (Lan et al., 2008). Furthermore, treatment of HepG2 cells with nicotinamide significantly inhibited the activity of Sirt1, thereby blocking AMPK phosphorylation and inhibiting lipolysis (Hou et al., 2008). Consistently, we also found that addition of the inhibitor of Sirt1 could abolish the activation effect of uridine in vitro. All these results showed that Sirt1 may be the upstream regulator of AMPK in the regulation of hepatocyte lipid metabolism with uridine addition.

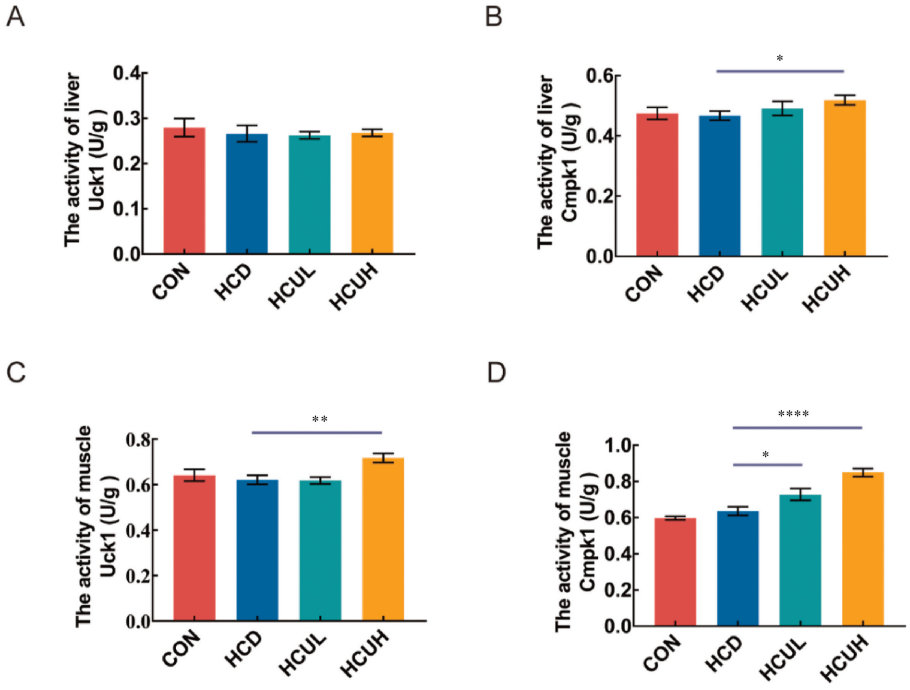

Fig. 3. The effect of uridine on activities of enzymes related to uridine metabolism in Nile tilapia. (A) The activity of liver Uck1 ($n = 6$). (B) The activity of liver Cmpk1 ($n = 6$). (C) The activity of muscle Uck1 ($n = 6$). (D) The activity of muscle Cmpk1 ($n = 6$). Data are represented as mean ± SEM. Significant difference compared with HCD (*$P < 0.05$, **$P < 0.01$, ****$P < 0.0001$). Uck1 = uridine–cytidine kinase 1; Cmpk1 = cytidine/uridine monophosphate kinase 1.

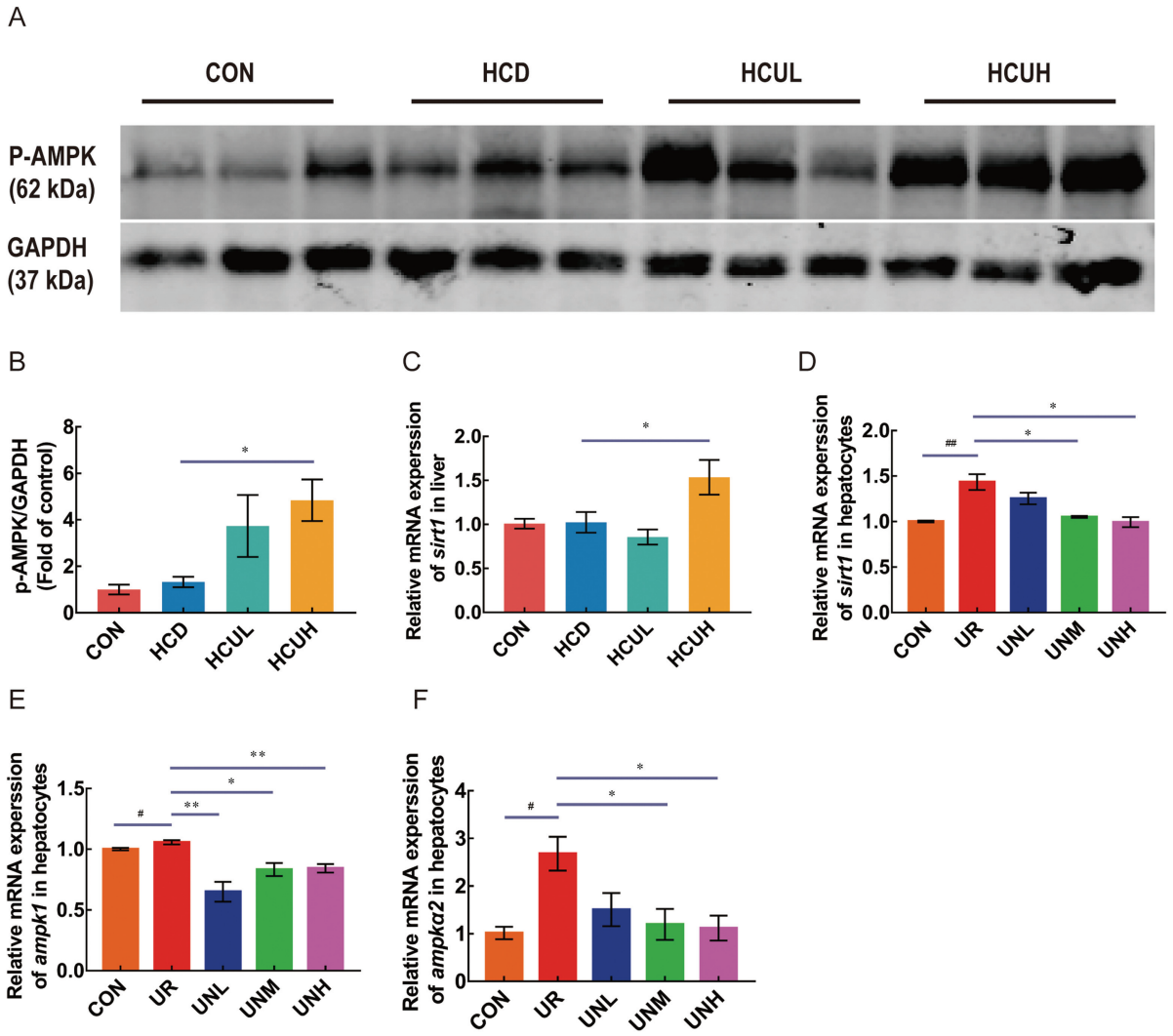

Fig. 4. The effects of uridine on the expression of AMPK protein and gene and the expression of *sirt1* gene in vivo and in vitro. (A) The protein expression of p-AMPK ($n = 3$). (B) Quantitation of the levels of p-AMPK was normalized to that of GAPDH ($n = 3$). (C) mRNA expression of *sirt1* in liver ($n = 6$). (D) Effect of uridine on the expression of *sirt1* in primary hepatocytes in the presence of nicotinamide ($n = 3$). (E) Effect of uridine on the expression of *ampkα1* in primary hepatocytes in the presence of nicotinamide ($n = 3$). (F) Effect of uridine on the expression of *ampkα2* in primary hepatocytes in the presence of nicotinamide ($n = 3$). Data are represented as mean ± SEM. (B–C): significant difference compared with HCD (*$P < 0.05$, **$P < 0.01$); (D–F): significant difference between CON and UR (#$P < 0.05$, ##$P < 0.01$); significant difference compared with UR (*$P < 0.05$, **$P < 0.01$). CON = control diet; HCD = high-carbohydrate diet; HCUL = high-carbohydrate diet + 500 mg/kg uridine; HCUH = high-carbohydrate diet + 5,000 mg/kg uridine; UR = hepatocytes treated with 500 μM uridine; UNL = hepatocytes treated with 500 μM uridine and 0.5 μM niacinamide; UNM = hepatocytes treated with 500 μM uridine and 1 μM niacinamide; UNH = hepatocytes treated with 500 μM uridine and 2 μM niacinamide. AMPK = adenosine 5-monophosphate-activated protein kinase; *sirt1* = sirtuin 1; *ampkα1* = AMP-activated protein kinase alpha 1; *ampkα2* = AMP-activated protein kinase alpha 2.

The previous study reported that administration of uridine to mice fed a high-fat diet significantly enhanced insulin sensitivity in a leptin-dependent manner (Deng et al., 2017). However, it has also been found that injection of uridine increased the level of UDP-N-acetylglucosamine, which induced insulin resistance (Hawkins et al., 1997). Our data showed dietary uridine significantly reduced the serum glucose but it had no effect on glucose tolerance and insulin content (data not shown), suggesting that the insulin signaling pathway may not be the main reason for the decreased serum glucose in the uridine addition groups. Activation of AMPK could enhance glycolysis (Steinberg and Kemp, 2009), and the present study indicated that a higher concentration of uridine activated AMPK to enhance hepatic glycolysis, which caused a decrease in serum glucose. On the other hand, serum glucose is the substrate for glycogen synthesis, and the level of serum glucose can be regulated by the metabolism of glycogen. Uridine is a precursor substance of UTP, which is required for the production of UDP-glucose and is involved in glycogen synthesis (Haugaard et al., 1977). In the present study, a higher concentration of uridine significantly activated glycogen synthesis in liver and muscle. The increased activity of glycogen synthetase and up-regulation of *ugp2* confirmed the effect of uridine on glycogen synthesis, which is consistent with the result in pancreatic ductal adenocarcinoma cells (Wolfe Andrew et al., 2021). Uck1 and Cmpk1 are the rate-limiting enzymes in uridine to UTP metabolism (Liou et al., 2002; Suzuki et al., 2004). In our study, a higher concentration of uridine significantly increased the activities of Uck1 and Cmpk1 in muscle and increased activity of Cmpk1 in liver, indicating enhanced synthesis of UTP in these 2 tissues. Consistently, uridine supplementation increased cellular UTP and stimulated glycogen synthesis in rats in vitro (Hawkins et al., 1997). Hence, addition of uridine increased glycolysis and induced glycogen synthesis to decrease the serum glucose.

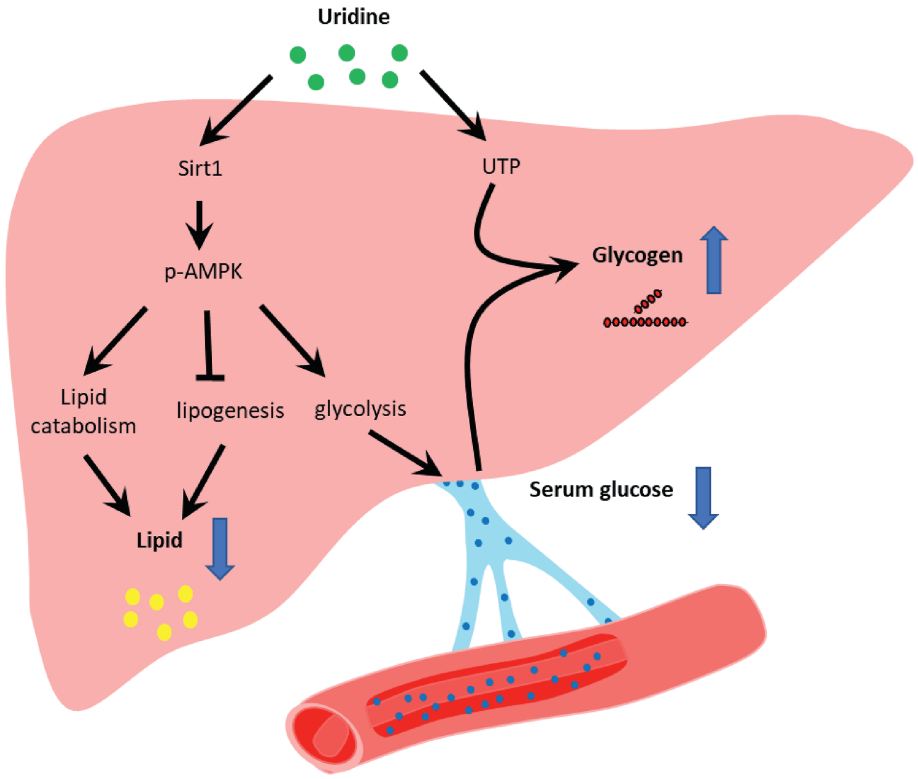

Fig. 5. The mechanism of uridine on glucose and lipid metabolism in Nile tilapia. Uridine intake by Nile tilapia activated sirt1 and then enhanced AMPK phosphorylation, which subsequently activated lipolysis, inhibited lipid synthesis, and promoted glycolysis, resulting in a decrease in liver lipid and serum glucose content. On the other hand, the increased synthesis of UTP after the intake of uridine in Nile tilapia further promotes the synthesis of glycogen, which helps to lower serum glucose content. sirt1 = sirtuin 1; AMPK = adenosine 5-monophosphate-activated protein kinase; UTP = uridine triphosphate.

5. Conclusions

It could be concluded that the addition of 5,000 mg/kg uridine to the diet inhibited lipogenesis and promoted lipid catabolism when Nile tilapia were fed with a HCD. To our knowledge, this study showed for the first time that uridine plays an important role in metabolic homeostasis for fish fed with HCD. The regulatory mechanism of uridine on glucose and lipid metabolism homeostasis in the background of a HCD is summarized in Fig. 5. In brief, uridine could alleviate HCD-induced metabolic syndromes by activating the sirt1/AMPK signaling pathway and promoting glycogen synthesis. This finding reveals the function of uridine in fish metabolism and facilitates the development of additives in aquatic feeds.

Author contributions

Nan-Nan Zhou: Conceptualization, Investigation, Formal analysis, Writing – Original draft, Visualization. **Tong Wang**: Methodology, Writing editing. **Yu-Xin Lin**: Resources, Data curation. **Rong Xu**: Project administration, Methodology. **Hong-Xia Wu**: Methodology, Formal analysis. **Fei-Fei Ding**: Methodology, Data curation. **Fang Qiao:** Conceptualization, Supervision. **Zhen-Yu Du**: Conceptualization, Supervision. **Mei-Ling Zhang**: Conceptualization, Project administration, Supervision, Writing – Reviewing and Editing.

Declaration of competing interest

We declare that we have no financial and personal relationships with other people or organizations that can inappropriately influence our work, and there is no professional or other personal interest of any nature or kind in any product, service and/or company that could be construed as influencing the content of this paper.

Acknowledgments

The authors appreciate the financial support provided by the National Key Research and Development Program (grant number: 2022YFD2400800) and National Natural Science Foundation of China (grant number: 31972798), and we thank the Instruments Sharing Platform of School of Life Sciences, East China Normal University for technical service.

References

Ali A, Al-Asgah NA. Effect of feeding different carbohydrate to lipid ratios on the growth performance and body composition of nile tilapia (*Oreochromis niloticus*) fingerlings. Anim Res 2001;50(1):91–100.
AOAC. Official methods of analysis. 18th ed. Arlington, VA, USA: Association of official Analytical Chemists; 2005.
Cantó C, Auwerx J. Targeting sirtuin 1 to improve metabolism: all you need is NAD(+)? Pharmacol Rev 2012;64:166–87.
Carling D. AMPK signalling in health and disease. Curr Opin Cell Biol 2017;45:31–7.
Cheng Z, Buentello A, Gatlin DM. Dietary nucleotides influence immune responses and intestinal morphology of red drum *Sciaenops ocellatus*. Fish Shellfish Immunol 2011;30:143–7.
Cool B, Zinker B, Chiou W, Kifle L, Cao N, Perham M, et al. Identification and characterization of a small molecule AMPK activator that treats key components of type 2 diabetes and the metabolic syndrome. Cell Metab 2006;3:403–16.
Daneshmand A, Kermanshahi H, Danesh Mesgaran M, King AJ, Ibrahim SA. Effects of pyrimidine nucleosides on growth performance, gut morphology, digestive enzymes, serum biochemical indices and immune response in broiler chickens. Livest Sci 2017;204:1–6.
Day EA, Ford RJ, Steinberg GR. AMPK as a therapeutic target for treating metabolic diseases. Trends Endocrinol Metab 2017;28:545–60.

Deng Y, Wang ZV, Gordillo R, Zhu Y, Ali A, Zhang C, et al. Adipocyte Xbp1s overexpression drives uridine production and reduces obesity. Mol Metabo 2018;11:1–17.
Deng YF, Wang ZV, Gordillo R, An Y, Zhang C, Liang QR, et al. An adipo-biliary-uridine axis that regulates energy homeostasis. Sci 2017;355.
Du ZY, Turchini GM. Are we actually measuring growth?—an appeal to use a more comprehensive growth index system for advancing aquaculture research. Rev Aquacult 2021;14:525–7.
FAO. The state of world fisheries and aquacult 2022. 2022.
Folch J, Lees M, Stanley GHS. A simple method for the isolation and purification of total lipides from animal tissues. J Biol Chem 1957;226:497–509.
Gao LM, Liu YL, Zhou XH, Zhang Y, Wu X, Yin YL. Maternal supplementation with uridine influences fatty acid and amino acid constituents of offspring in a sow-piglet model. Br J Nurt 2021;125:743–56.
Haugaard ES, Frantz KB, Haugaard N. Effect of uridine on cellular UTP and glycogen synthesis in skeletal muscle: stimulation of UTP formation by insulin. Proc Natl Acad Sci 1977;74:2339–42.
Hawkins M, Angelov I, Liu R, Barzilai N, Rossetti L. The tissue concentration of UDP-N-acetylglucosamine modulates the stimulatory effect of insulin on skeletal muscle glucose uptake. J Biol Chem 1997;272:4889–95.
Hou X, Xu S, Maitland-Toolan KA, Sato K, Jiang B, Ido Y, et al. SIRT1 regulates hepatocyte lipid metabolism through activating AMP-activated protein kinase. J Biol Chem 2008;283:20015–26.
Jéquier E. Carbohydrates as a source of energy. Am J Clin Nutr 1994;59:682S–5S.
Jiao J-G, Liu Y, Zhang H, Li L-Y, Qiao F, Chen L-Q, et al. Metabolism of linoleic and linolenic acids in hepatocytes of two freshwater fish with different n-3 or n-6 fatty acid requirements. Aquaculture 2020;515:734595.
Kahn BB, Alquier T, Carling D, Hardie DG. AMP-activated protein kinase: ancient energy gauge provides clues to modern understanding of metabolism. Cell Metab 2005;1:15–25.
Lan F, Cacicedo JM, Ruderman N, Ido Y. SIRT1 modulation of the acetylation status, cytosolic localization, and activity of LKB1: possible role in AMP-activated protein kinase activation. J Biol Chem 2008;283:27628–35.
Le TT, Urasaki Y, Pizzorno G. Uridine prevents fenofibrate-induced fatty liver. PLoS One 2014a;9.
Le TT, Urasaki Y, Pizzorno G. Uridine prevents tamoxifen-induced liver lipid droplet accumulation. BMC Pharmacol and Toxicol 2014b;15:27.
Le TT, Ziemba A, Urasaki Y, Hayes E, Brotman S, Pizzorno G. Disruption of uridine homeostasis links liver pyrimidine metabolism to lipid accumulation. J Lipid Res 2013;54:1044–57.
Li Y, Xu SQ, Mihaylova MM, Zheng B, Hou XY, Jiang BB, et al. AMPK phosphorylates and inhibits SREBP activity to attenuate hepatic steatosis and atherosclerosis in diet-induced insulin-resistant mice. Cell Metab 2011;13:376–88.
Liang C, Curry BJ, Brown PL, Zemel MB. Leucine modulates mitochondrial biogenesis and SIRT1-AMPK signaling in C2C12 myotubes. J Nutr Metab 2014;2014:239750.
Lin S-M, Shi C-M, Mu M-M, Chen Y-J, Luo L. Effect of high dietary starch levels on growth, hepatic glucose metabolism, oxidative status and immune response of juvenile largemouth bass, *Micropterus salmoides*. Fish Shellfish Immunol 2018;78:121–6.
Lin YH, Wang H, Shiau SY. Dietary nucleotide supplementation enhances growth and immune responses of grouper, *Epinephelus malabaricus*. Aquacul Nutr 2009;15:117–22.
Liou JY, Dutschman GE, Lam W, Jiang ZL, Cheng YC. Characterization of human UMP/CMP kinase and its phosphorylation of D- and L-form deoxycytidine analogue monophosphates. Cancer Res 2002;62:1624–31.
Liu XJ, Luo Z, Xiong BX, Liu X, Zhao YH, Hu GF, et al. Effect of waterborne copper exposure on growth, hepatic enzymatic activities and histology in *Synechogobius hasta*. Ecotoxicol Environ Saf 2010;73:1286–91.
Liu YL, Xie CY, Zhai ZY, Deng ZY, De Jonge HOR, Wu X, et al. Uridine attenuates obesity, ameliorates hepatic lipid accumulation and modifies the gut microbiota composition in mice fed with a high-fat diet. Food Funct 2021;12:1829–40.
Michailidou F, Burnett D, Sharma SV, Van Lanen SG, Goss RJM. 2.19 - natural products incorporating pyrimidine nucleosides. In: Liu H-W, Begley TP, editors. Comprehensive natural products III. Oxford: Elsevier; 2020. p. 500–36.
Musso G, Gambino R, Cassader M. Recent insights into hepatic lipid metabolism in non-alcoholic fatty liver disease (NAFLD). Prog Lipid Res 2009;48:1–26.
Panserat S, Kaushik S. Nutritional regulation of hepatic glucose metabolism in fish: example of a poor user of dietary carbohydrates, the rainbow trout. Prod Anim 2002;15:109–17.
Peng K, Wang G, Zhao H, Wang Y, Mo W, Wu H, et al. Effect of high level of carbohydrate and supplementation of condensed tannins on growth performance, serum metabolites, antioxidant and immune response, and hepatic glyco-metabolism gene expression of *Lateolabrax japonicus*. Aquacul Rep 2020;18:100515.
Peng M, Xu W, Ai Q, Mai K, Liufu Z, Zhang K. Effects of nucleotide supplementation on growth, immune responses and intestinal morphology in juvenile turbot fed diets with graded levels of soybean meal (*Scophthalmus maximus L.*). Aquaculture 2013;392–395:51–8.
Shi H-J, Xu C, Liu M-Y, Wang B-K, Liu W-B, Chen D-H, et al. Resveratrol improves the energy sensing and glycolipid metabolism of blunt snout bream *Megalobrama amblycephala* fed high-carbohydrate diets by activating the AMPK–SIRT1–PGC-1α Network. Front Physiol 2018;9.
Steinberg GR, Kemp BE. AMPK in health and disease. Physiol Rev 2009;89:1025–78.
Suzuki NN, Koizumi K, Fukushima M, Matsuda A, Inagaki F. Structural basis for the specificity, catalysis, and regulation of human uridine-cytidine kinase. Struct 2004;12:751–64.
Tahmasebi-Kohyani A, Keyvanshokooh S, Nematollahi A, Mahmoudi N, Pasha-Zanoosi H. Dietary administration of nucleotides to enhance growth, humoral immune responses, and disease resistance of the rainbow trout (*Oncorhynchus mykiss*) fingerlings. Fish Shellfish Immunol 2011;30:189–93.
Takikawa M, Inoue S, Horio F, Tsuda T. Dietary anthocyanin-rich bilberry extract ameliorates hyperglycemia and insulin sensitivity via activation of AMP-activated protein kinase in diabetic mice. J Nutr 2010;140:527–33.
Urasaki Y, Pizzorno G, Le TT. Chronic uridine administration induces fatty liver and pre-diabetic conditions in mice. PLoS One 2016;11.
Wang T, Zhang N, Yu X-B, Qiao F, Chen L-Q, Du Z-Y, et al. Inulin alleviates adverse metabolic syndrome and regulates intestinal microbiota composition in Nile tilapia (*Oreochromis niloticus*) fed with high-carbohydrate diet. Br J Nutr 2021;126:161–71.
Welker TL, Lim C, Yildirim-Aksoy M, Klesius PH. Effects of dietary supplementation of a purified nucleotide mixture on immune function and disease and stress resistance in channel catfish, *Ictalurus punctatus*. Aquacul Res 2011;42:1878–89.
Wolfe Andrew L, Zhou Q, Toska E, Galeas J, Ku Angel A, Koche Richard P, et al. UDP-glucose pyrophosphorylase 2, a regulator of glycogen synthesis and glycosylation, is critical for pancreatic cancer growth. Proc Natl Acad Sci 2021;118:e2103592118.
Wu X, Gao L-M, Liu Y-L, Xie C, Cai L, Xu K, et al. Maternal dietary uridine supplementation reduces diarrhea incidence in piglets by regulating the intestinal mucosal barrier and cytokine profiles. J Sci Food Agric 2020;100:3709–18.
Xu C, Liu W-B, Zhang D-D, Cao X-F, Shi H-J, Li X-F. Interactions between dietary carbohydrate and metformin: Implications on energy sensing, insulin signaling pathway, glycolipid metabolism and glucose tolerance in blunt snout bream *Megalobrama amblycephala*. Aquaculture 2018;483:183–95.
Xu R, Wang T, Ding F-F, Zhou N-N, Qiao F, Chen L-Q, et al. Lactobacillus plantarum ameliorates high-carbohydrate diet-induced hepatic lipid accumulation and oxidative stress by upregulating uridine synthesis. Antioxidants 2022:11.
Xu R, Li M, Wang T, Zhao Y-W, Shan C-J, Qiao F, et al. Bacillus amyloliquefaciens ameliorates high-carbohydrate diet-induced metabolic phenotypes by restoration of intestinal acetate-producing bacteria in Nile Tilapia. Br J Nutr 2022b;127:653–65.
Yamamoto T, Koyama H, Kurajoh M, Shoji T, Tsutsumi Z, Moriwaki Y. Biochemistry of uridine in plasma. Clin Chim Acta 2011;412:1712–24.
Yao H, Tao X, Xu L, Qi Y, Yin L, Han X, et al. Dioscin alleviates non-alcoholic fatty liver disease through adjusting lipid metabolism via SIRT1/AMPK signaling pathway. Pharmacol Res 2018;131:51–60.
Zhang Y, Guo S, Xie C, Fang J. Uridine metabolism and its role in glucose, lipid, and amino acid homeostasis. BioMed Res Int 2020;2020:7091718.
Zhao W, Xie J-J, Fang H-H, Liu Y-J, Tian L-X, Niu J. Effects of corn starch level on growth performance, antioxidant capacity, gut morphology and intestinal microflora of juvenile golden pompano, *Trachinotus ovatus*. Aquaculture 2020;524:735197.